Environmental Science Advances

ROYAL SOCIETY OF CHEMISTRY

PAPER

View Article Online
View Journal | View Issue

Cite this: *Environ. Sci.: Adv.*, 2024, **3**, 1735

"Tree of life": how baobab seed-derived biochar could lead to water safety for underprivileged communities through heavy metal (Fe) removal – SDG 6

Magdalena J. Mkelemi, Grite N. Mwaijengo and Mwemezi J. Rwiza *

The abnormally gigantic baobab tree (*Adansonia digitata*) is often referred to as the "Tree of Life" due to its ability to provide food, water, shelter, and traditional medicine for both humans and animals in arid regions. This special tree is a landmark of Africa's savanna and has attracted the attention of the global research community. This study investigated the potential of biochar derived from baobab seeds for the removal of metallic ions from groundwater. The biochar, prepared at 700 °C, exhibited a unique surface morphology with deep voids and varied structures, suggesting increased surface area and favorable conditions for adsorption. SEM-EDX analyses confirmed the elemental composition, with carbon being the predominant element. Furthermore, XRD analysis indicated an amorphous structure, enhancing adsorption capacity for heavy metal ions. Additionally, BET analysis revealed a significant surface area (1386.704 m^2 g^{-1}) and well-defined pores, emphasizing the material's potential for metallic ion removal. The metallic ion of choice for this research was Fe because of its abundance in the study area and the community's need for affordable technology for discoloration of reddish-brown groundwater caused by Fe ion presence. In the batch mode equilibrium studies, the effect of pH, contact time, adsorbent particle size, adsorbent dose, solution temperature, and initial metal ion concentration was investigated. Optimal pH metallic ion removal occurred under neutral pH conditions, with higher removal efficiency observed at increased contact time (up to 120 min) and adsorbent doses. Adsorption isotherm modeling using Langmuir and Freundlich models indicated favorable adsorption, with the Freundlich model providing a slightly better fit. In conclusion, baobab seed-derived biochar demonstrated promising potential as an efficient and sustainable adsorbent for metal ion removal from groundwater. Further exploration, including the development of activated carbon and field applications, is recommended for a comprehensive understanding and practical optimization of this material's capabilities for metal ion removal.

Received 15th June 2024
Accepted 24th September 2024

DOI: 10.1039/d4va00205a

rsc.li/esadvances

Environmental significance

This study highlights the innovative use of baobab seed-derived biochar as a sustainable solution for purifying groundwater by removing metallic ions, specifically iron, which causes coloration and potential health issues. The research demonstrates that baobab seed-derived biochar, with its unique surface properties and high adsorption capacity, offers an environmentally friendly and cost-effective method for communities in arid regions to access clean water. This advancement aligns with global efforts to ensure water security and protect ecosystems (for example the Sustainable Development Goal number 6 – SDG 6), showcasing the baobab tree's continued significance as the "Tree of Life."

Introduction

The baobab tree (*Adansonia digitata* L.) is widely distributed across sub-Saharan Africa,[1] with countries like Tanzania, especially in arid regions like Dodoma and Singida, cultivating it. Baobab seeds are recognized for their effective removal of turbidity from water; however, they may introduce organic nutrients, impacting water quality.[2] In response to this, the study focused on utilizing biochar derived from baobab seeds, taking into consideration the economic and social significance of the baobab tree in rural areas. Through pyrolysis, baobab seeds can be transformed into biochar, a carbon-rich material known for its high surface area and adsorption capabilities. This approach aims to enhance adsorption capabilities, and eliminate organic compounds,[3] thereby addressing a research

School of Materials, Energy, Water and Environmental Sciences (MEWES), The Nelson Mandela African Institution of Science and Technology (NM-AIST), P.O. Box 447, Arusha, Tanzania. E-mail: mwemezi.rwiza@nm-aist.ac.tz

gap, and provide a potential solution for effective Fe removal from groundwater.[2]

The significance of water for human health and well-being is undeniable, and maintaining its quality is crucial in various applications such as agricultural, domestic, industrial and commercial uses.[2] Groundwater, due to its accessibility and relative protection against pollution, is widely used for large-scale water supply worldwide.[4] However, both groundwater and surface water sources encounter challenges from organic and inorganic chemical contamination, with groundwater often experiencing elevated levels of heavy metals, including Fe, being a common one.[5]

Fe contamination in groundwater is a widespread issue, often arising from natural geological processes or anthropogenic activities.[6] Excessive Fe levels not only lead to undesirable taste and discoloration but can also result in serious health concerns, including gastrointestinal problems and increased susceptibility to waterborne diseases.[7] Fe exists in two forms, ferrous and ferric Fe.[7] Heavy metals are as a result of natural occurrences in the earth's crust or introduced through human activities like waste disposal, mining and industrial processes. Groundwater, naturally occurring in aquifers, percolates through rocks and subsurface soil, potentially dissolving metals found in rocks.[5] While some metals, like Fe, are beneficial in limited quantities, elevated concentrations beyond the WHO's recommended limit of 0.3 mg L^{-1} result in aesthetic problems and indirect health issues.[8] The excess Fe imparts reddish-brown colour, produces a metallic taste and unpleasant odour, and stains surfaces.[9] Additionally, the accumulation of Fe in pipes causes practical issues such as restricted water flow, decreased pressure, and heightened energy requirements for water treatment.[8]

Various treatment methods such as oxidation filtration, ion exchange, coagulation/flocculation, aeration, reverse osmosis, greensand, polyphosphates and chemical filtration, have been reported to address Fe contamination in water.[10] The choice of method depends on the type and concentration of Fe present.[10] Oxidation and filtration, for example, involves oxidizing soluble ferrous Fe to insoluble ferric Fe, with air and chlorine as common oxidizing agents.[9] However, practical challenges limit the application of many of these methods in rural areas.[2]

Adsorption technologies have gained attention due to their simplicity and effectiveness.[11] Numerous studies have extensively investigated the use of adsorbents conducted on the use of adsorbents such as modified agricultural residues, activated carbon, zeolites, natural clay minerals for Fe removal from water.[11–15] The efficacy of an adsorbent relies on its surface adsorptive properties, wherein adsorption occurs when a solid surface contacts a solution, accumulating a surface layer of solute molecules due to imbalanced surface forces.[16]

The current study aims to assess the potential use of baobab seed-derived biochar for efficient Fe removal from groundwater, considering the widespread distribution of baobab trees in sub-Saharan Africa, particularly in Tanzania.[1] To check the adsorbent effectiveness, the adsorbent was characterized using Scanning Electron Microscopy-Energy Dispersive Spectroscopy (SEM-EDS), X-Ray Diffraction (XRD) and Brunauer Emmett Teller (BET) analysis. Batch tests investigated the ferrous adsorption capacity onto baobab seed-derived biochar, employing empirical models and adsorption isotherms like Freundlich and Langmuir. Although linear models used for this study suffer from inherent weaknesses,[17] some scholars *e.g.*, Ayawei *et al.* (2017) have insisted that these linearized models can still provide useful information related to the distribution of adsorbates, insights related to the adsorption system, and the confirmation of the consistency of theoretical assumptions.[18]

Materials and methods

Collection and preparation of the adsorbent

This study utilized biochar derived from baobab seeds (*Adansonia digitata* L.) as an adsorbent to remove Fe from water. The baobab seeds, sourced locally and commercially available, underwent a rigorous cleaning process with distilled water to eliminate surface impurities. Subsequently, the seeds were sun-dried for 2 days and air-dried at 105 °C in a hot air oven and subjected to carbonation (pyrolysis) in a Gallonhop muffle furnace at temperatures ranging from 400 to 700 °C for 2.5 hours, with a controlled temperature increase of 8–10 °C min^{-1}. Following a 20-minute residence time, the furnace was gradually cooled to 40–50 °C. The resulting carbonized seeds were finely ground to fine powder using a blender, sieved through a 90 μm mesh, and stored in an airtight plastic container for future applications. This methodology aligns with the work of Tabassum *et al.* (2019)[19] with little modifications.

Collection of the groundwater water sample

The groundwater sample was collected from the borehole at Ilembo village in Mpanda district using polyethylene containers at Latitude 11°8′4.39″ N and Longitude 7°39′26.24″ E. The actual location of collection was determined using Global Positioning System (GPS). The first 50–100 mL of sample was used to rinse the containers first before the required volume was collected. The initial Fe of groundwater water was about 6.0 mg L^{-1}.

Preparation of synthesized Fe-contaminated water

In the preparation of synthesized Fe-contaminated water, Fe sulphate salt was employed to achieve different initial Fe concentrations ranging from 2 g L^{-1} to 30 g L^{-1}. Deionized water was utilized in the process, with the exact volume required added to a 1000 mL volumetric flask. Thorough mixing ensured a homogenous solution at each concentration level. The varied amounts of iron sulphate salt allowed for the creation of a series of water samples with precisely controlled Fe concentrations, facilitating subsequent experiments and analyses related to Fe contamination.

Jar test experiments for Fe removal

The study systematically explores the influence of varying doses of the adsorbent on the removal of Fe from untreated field water. Jar test experiments were conducted using a flocculator (PCI Ltd, England). Six 1000 mL water beakers were filled with

contaminated water, and adsorbent doses of 0.6 g L^{-1}, 1.2 g L^{-1}, 1.8 g L^{-1}, 2.4 g L^{-1}, and 3.0 g L^{-1} were added, with one water beaker serving as a control. A stirring machine ensured consistent mixing of water and the adsorbent, involving 3 minutes of rapid mixing at 100 rpm followed by 17 minutes of slow mixing at 30 rpm. Subsequently, the samples underwent filtration using Whatman paper No. 1, and the filtrate was analysed using a DR6000 spectrophotometer to determine residual Fe concentrations. The entire experimental procedure was repeated thrice for reliability and reproducibility, and obtained values were computed to get the averages.

The study also investigated the impact of adsorption temperature, solution pH, adsorbent particle size, initial Fe concentration, and contact time on Fe removal in the jar test experiment. For the adsorption temperature study, experiments were conducted at temperatures ranging from 20 °C (293.15 K) to 50 °C (323.15 K) while keeping other parameters constant. The effect of solution pH on Fe ion removal was investigated by adjusting the pH from 2.0 to 12.0 using 0.1 M hydrochloric acid (HCl) or 0.1 M sodium hydroxide (NaOH). Particle size analysis involved sieving the adsorbent through different sizes (90 μm to 1000 μm), maintaining a constant dose and other parameters. Additionally, the impact of initial Fe concentration and contact time on adsorption uptake was explored by preparing 1000 mL adsorbate solutions with initial Fe concentrations ranging from 2 to 30 mg L^{-1}. In each solution, the adsorbent (baobab seed-derived biochar) was added, and jar tests were conducted at a constant temperature of 25 °C with a rotation speed of 100 rpm for 2.5 hours.

The Fe removal efficiency (Re) was determined using eqn (1):

$$\%\mathrm{Re} = \frac{C_o - C_t}{C_o} \times 100 \quad (1)$$

where % Re represents the removal efficiency and C_o and C_t (mg L^{-1}) denote the initial and time t concentrations of Fe, respectively.

Additionally, the sorption capacity (q_t) was calculated using eqn (2):

$$q_t = \frac{C_o - C_t \times V}{m} \quad (2)$$

where, q_t represents the sorption capacity, V represents the volume of liquid phase (L), and m (g) is the weight of the baobab seed adsorbent.

Thermodynamic parameter calculations

In this study, thermodynamic parameters such as the equilibrium constant (K), Gibbs free energy (ΔG), enthalpy (ΔH), and entropy (ΔS) were determined based on adsorption data at varying temperatures.

The equilibrium constant (K), which in this context is represented by the Langmuir constant (K_L), was calculated using the Langmuir isotherm model. The linearized Langmuir isotherm equation is given by eqn (3):

$$\frac{C_e}{q_e} = \frac{1}{q_m K_L} + \frac{C_e}{q_m} \quad (3)$$

where, C_e is the equilibrium concentration of the adsorbate (mg L^{-1}), q_e is the amount of adsorbate adsorbed per unit mass of the adsorbent at equilibrium (mg g^{-1}), q_m is the maximum adsorption capacity (mg g^{-1}), and K_L is the Langmuir constant (L mg^{-1}).

To determine K_L, a plot of C_e/q_e *versus* C_e was constructed. The slope of the linear plot corresponds to $1/q_m$, and the intercept is $1/q_m \times K_L$. Using these, the Langmuir constant K_L was calculated using eqn (4):

$$K_L = \frac{\text{slope}}{\text{intercept}} \quad (4)$$

Once K_L was calculated for each temperature, the Gibbs free energy change (ΔG) was determined using the thermodynamic eqn (5):

$$\Delta G = -RT \ln K \quad (5)$$

where R is the universal gas constant (8.314 J mol^{-1} K^{-1}), T is the absolute temperature (K), and K is the equilibrium constant (calculated as K_L).

A negative value of ΔG indicates that the adsorption process is spontaneous, while a positive value suggests non-spontaneity. The values of ΔG were calculated for each temperature to analyse how temperature affects the spontaneity of the process.

To further examine the thermodynamic behaviour, the enthalpy change (ΔH) and entropy change (ΔS°) were calculated using the Van't Hoff eqn (6):[20]

$$\ln K = -\frac{\Delta H^\circ}{R} \cdot \frac{1}{T} + \frac{\Delta S^\circ}{R} \quad (6)$$

where K is the equilibrium constant, ΔH° represents the standard enthalpy of formation, R is a gas constant, T denotes the reaction temperature (in K), and ΔS° represents the standard entropy.

A plot of $\ln K$ *versus* $1/T$ provided a straight line, with the slope of the line corresponding to $-\Delta H^\circ/R$ and the intercept corresponding to $\Delta S/R$. From this, ΔH and ΔS were calculated.

Enthalpy change (ΔH°) reflects the heat absorbed or released during adsorption. A positive ΔH indicates an endothermic process, meaning heat is absorbed, while a negative ΔH indicates an exothermic process, meaning heat is released.

Entropy change (ΔS°) represents the change in disorder or randomness at the solid–liquid interface. A positive ΔS° indicates an increase in randomness, which generally favors adsorption, while a negative ΔS° suggests a decrease in disorder.

Characterization of baobab seed-derived biochar

The morphological characteristics of the adsorbent, baobab seed-derived biochar, were investigated using a ZEISIS SIGMA 300 VP scanning electron microscope (SEM) coupled with a Smart EDX. To prevent charge accumulation during measurement, the samples were placed on double-sided carbon conductive tape and double-coated with a carbon layer using a Quorum Q150T ES instrument. Additionally, Shimadzu X-ray

diffraction patterns for baobab seed-derived biochar were obtained using a Pan-Analytical Goniometer with a Cu Kα radiation source. The scanning range was 5–80° over a 2-minute period at 30 kV and 15 mA.

The textural properties of baobab seed-derived biochar were determined through nitrogen sorption at −77 K after degassing the samples at 160 °C for 4 hours. The Quanta-chrome NOVA 1200e Series pore size and surface area analyser was employed, with the specific surface area (SBET) calculated using the Brunauer–Emmett–Teller (BET) method. The total pore volume (VT) was estimated based on the nitrogen adsorbed at a relative pressure of $P/P_0 \times 0.99$.

Statistical analysis

The information obtained from the experimental procedures were statistically analysed utilizing the IBM SPSS version 27.0 software. Each experiment was conducted three times for accuracy, and the average values were calculated along with standard deviations being determined.

Results and discussion

Characterization of the biochar adsorbent

SEM-EDX characterization. The study employed scanning electron microscopy (SEM) to scrutinize the surface morphology of biochar derived from baobab seeds, which was prepared at 700 °C. The SEM micrographs (Fig. 1), revealed distinctive features of the biochar, characterized by deep irregular voids, a rough surface and varied surface morphology. These structural attributes could have contributed to a heightened surface area, which is an indicator of more sites available for the adsorption of Fe ions and other contaminants present in water. Unlike for this study, other scholars such as Ealias and Saravanakumar[21] have, through transmission electron microscopy (TEM), conducted selected area electron diffraction (SAED) to substantiate diffraction conditions for adsorbent materials. The existence of both micro and mesopores in this study further implies an advantageous setting for the entrapment and adsorption of Fe ions from water.

These findings are supported by prior studies on activated carbon derived from orange peel which emphasized the consistency of the observed structural characteristics for adsorption of metal ions from water.[22] Furthermore, the Energy Dispersive X-ray (EDX) micrograph presented in Fig. 1 supplements the microscopic analysis by confirming the elemental

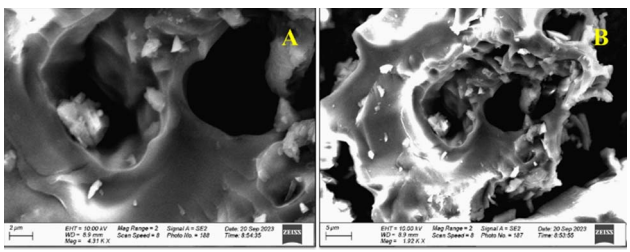

Fig. 1 (A and B) Scanning electron microscopy (SEM) micrographs of baobab seed-derived biochar at 700 °C.

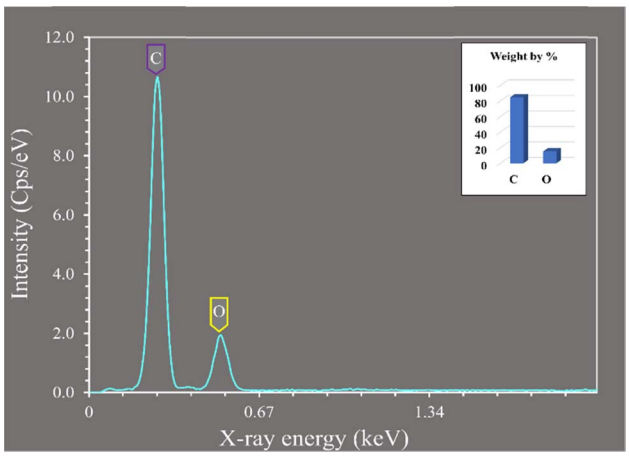

Fig. 2 The EDX micrograph illustrates the existence of carbon and oxygen in the biochar derived from baobab seeds after pyrolysis at 700 °C.

composition of the biochar prepared from baobab seeds. Carbon constituted the predominant element, comprising approximately 84.74%, followed by oxygen at 15.26% (Fig. 2). The present study was consistent with other prior research on activated carbon from *Jatropha curcas* used for decontamination of water, which identified a composition of 93.36% carbon and 6.64% oxygen in the activated carbon.[23]

In conclusion from this part, the comprehensive examination of the baobab seed-derived biochar, as supported by SEM-EDX analyses, substantiates its suitability for Fe adsorption. The distinct morphology, characterized by deep voids and well-developed pores, establishes the biochar as a promising adsorbent for the targeted removal of Fe ions from water.

X-ray diffraction (XRD). The crystal structure and mineral composition of biochar derived from baobab seeds were investigated through X-ray diffraction (XRD) analysis. Fig. 3 illustrates the XRD patterns, which revealed a distinct absence of well-defined peaks in any phase, indicating an amorphous structure without discrete mineral peaks. Notably, the 18–30 2θ degree range exhibited a pronounced hump, which might be a characteristic feature of a high degree of disorder commonly found in carbonaceous materials. The amorphous regions often have higher surface areas and exhibit enhanced adsorption

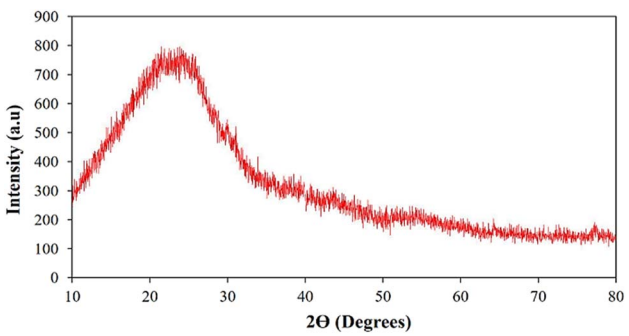

Fig. 3 The X-ray diffraction (XRD) of the biochar derived from baobab seeds.

capacities for heavy metal ions particularly Fe ions. These observations are consistent with previous studies on activated carbon derived from agricultural wastes, underlining the prevalent amorphous nature in such carbonaceous materials.[3,24]

Brunauer–Emmett–Teller (BET) analysis. In this study, the nitrogen adsorption/desorption isotherm was employed to determine the porosity of a synthesized carbonaceous adsorbent derived from baobab seed biochar focusing on surface area, pore size, and pore volume. The BET analysis, performed at 77 K, yielded insightful results presented in Fig. 4, depicting the sorption/desorption volume (Va/cm^3) of nitrogen gas against relative pressure (p/p_o).

The isotherms obtained displayed a linear relationship, particularly at low pressure, characteristic of the BET adsorption isotherm. This observation aligns with the theory's premise of monolayer adsorption on a homogeneous surface, typical of microporous materials. The straight-line behaviour underscores the formation of a monolayer of adsorbed molecules on the solid material's surface under ideal conditions. However, deviations from linearity were observed during desorption at higher pressures, suggesting potential multilayer adsorption or surface heterogeneity. This deviation could indicate the presence of mesopores in addition to micropores. The biochar exhibited a mean pore diameter of 3.742 nm, falling within the typical range for micropores, supporting its microporous nature.[25] The pore volume of 0.402 $cm^3\ g^{-1}$ provides insights into the total volume of pores, contributing to our understanding of material porosity.

The substantial BJH surface area of 1386.704 $m^2\ g^{-1}$, as determined by the BET analysis, implies a high degree of porosity and suggests a significant number of active sites available for adsorption reactions.[25] The slope of the linear portion of the isotherm is indicative of the specific surface area, with a steeper slope corresponding to a higher surface area.[26]

Equilibrium studies in batch mode

Effect of pH on Fe removal. The influence of pH on the adsorption of metal ions, particularly Fe, from aqueous solutions is a critical factor in the efficiency of the process. This is due to its impact on various aspects, including the solubility of Fe ions, the concentration of counter ions on the functional groups of the adsorbent and the ionization degree of the adsorbate during the reaction.[3,27] In a controlled study maintaining parameters such as adsorbent dose (3 g L^{-1}), agitation speed (120 rpm), solution temperature (25 ± 0.5 °C), adsorbent particle size (90 μm), initial Fe concentration (5.88 mg L^{-1}), and the impact of pH (ranging from 3.0 to 12.0) was examined. The results, as illustrated in Fig. 5, highlighted that the optimal adsorption of Fe occurred within the pH range of 5.0–8.0, with the highest adsorption capacity observed at pH 7.0, representing the neutral pH range typical for drinking water. Fe adsorption increased from pH 3 to 8 but decreased with further pH increase. A similar trend reported in ref. 28 demonstrated an increase in adsorption capacity from pH 2 to 8, followed by a decrease from pH 10 to 12. This phenomenon is explained by the precipitation of less soluble ferric hydroxide, creating a conducive environment for the formation of Fe $(OH)_3$, which is effectively adsorbed by the baobab seed biochar adsorbent. However, beyond a certain pH, the solubility of Fe species increases, thereby diminishing the efficacy of the adsorption process. The optimal pH for effective Fe removal is typically 5–8, with a decline observed at pH ≥9 due to hydroxide ion competition, negatively charged baobab seed surface under alkaline conditions, and prevalence of dominant negatively charged species.

Effect of contact time on Fe removal. The extraction of Fe from field groundwater was conducted across various contact times, ranging from 20 to 120 minutes, with an initial concentration of 5.88 mg L^{-1} in 100 mL solution flasks. Key operating parameters, including baobab seed-derived biochar (adsorbent) dose (3 g L^{-1}), agitation speed (120 rpm), room temperature (25 ± 0.5 °C), adsorbent particle size (90 μm), and solution pH of 7.0, were kept constant. The results presented in Fig. 6 show that the adsorption capacity increased with an increase in contact time up to 120 min. The observed percentage removal and uptake capacity of Fe by baobab seed-derived biochar exhibited a notable increase with prolonged reaction times, reaching an optimal removal efficiency of 87%, within 120

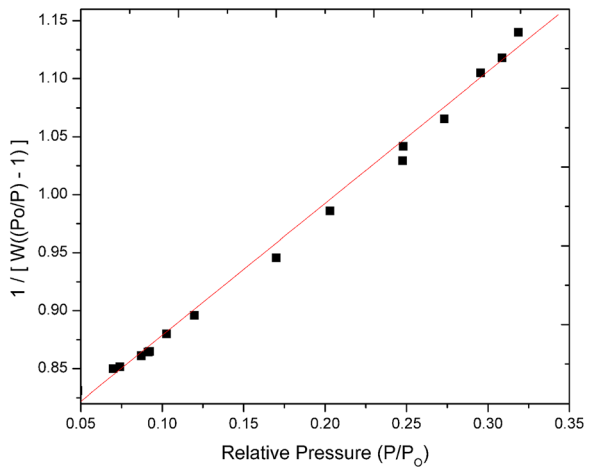

Fig. 4 Adsorption–desorption plot of N_2 at 77.35 K for baobab seed-derived biochar.

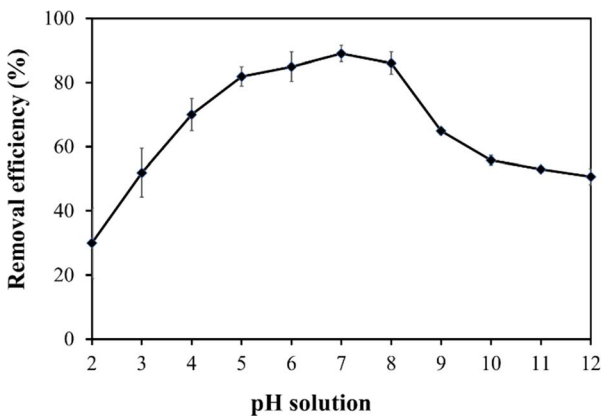

Fig. 5 Effect of pH on the % removal of Fe from the solution.

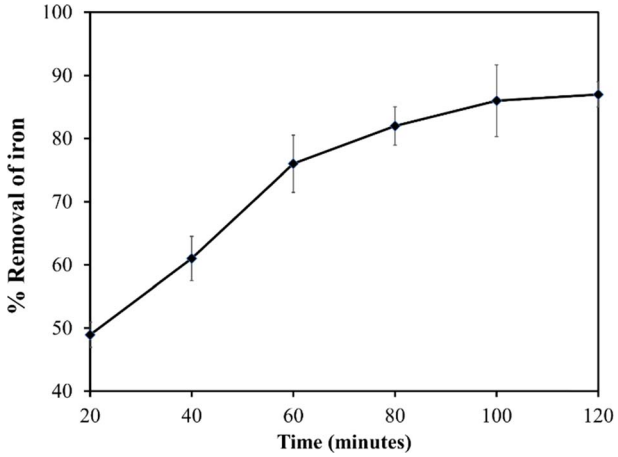

Fig. 6 Effect of contact time on % removal of Fe from aqueous solution.

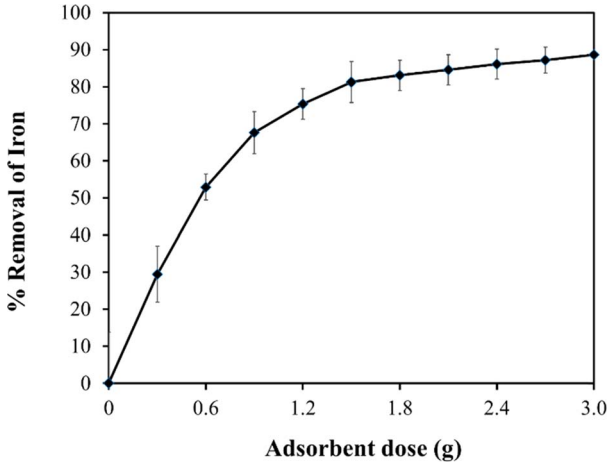

Fig. 8 Effect of adsorbent dose on Fe removal from groundwater.

minutes. Subsequently, the system reached equilibrium, indicating a stabilization in removal efficiency, as illustrated in Fig. 6. The reason for this observation is that at the beginning of the adsorption process, all the adsorption sites on the surface of the pyrolysis biochar were vacant and hence solute concentration gradient was relatively high. Subsequently after attaining equilibrium, the extent of Fe ion removal remained constant with increase in contact time, which is dependent on the number of vacant sites on the surface of the pyrolysis biochar.

Effect of particle size on Fe removal. The study investigated the influence of baobab seed-derived biochar adsorbent particle size on the removal of Fe from groundwater. Experiments were conducted with varying particle sizes (ranging from 90 to 1000 μm), maintaining constant conditions such as 120 rpm agitation speed, 5.88 mg L^{-1} initial Fe concentration, 25 ± 0.5 °C solution temperature, pH values of 7, adsorbent dose of 3.0 g and a 120-minute agitation time for de-polluting Fe ions from the Fe water.

The experimental results, illustrated in Fig. 7, revealed a decrease in the percentage removal of Fe ions by the adsorbent as particle size increased. This indicates that larger particle sizes of biochar were less effective in removing Fe from the water. The findings align with previous research,[29] suggesting that reducing the particle size enhances metal ion uptake. This improvement is attributed to the increased access to pores and a larger surface area for bulk sorption per unit weight of the baobab seed adsorbent.

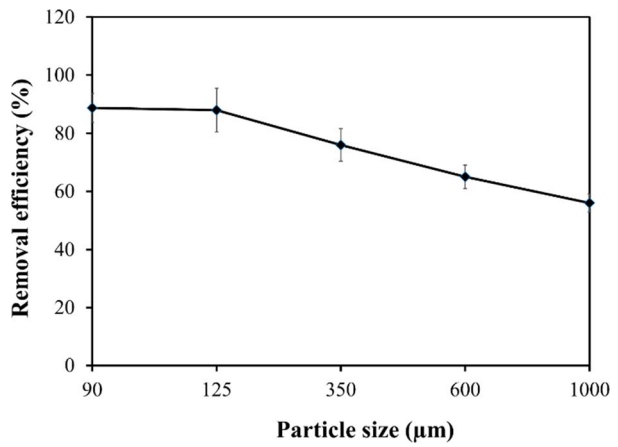

Fig. 7 Effect of contact time on % removal of Fe removal from groundwater.

Effect of adsorbent dose on Fe removal. This research also assessed how varying the dosage of a baobab seed-derived biochar (adsorbent) impacted the detoxification of Fe in water. The experiments involved different adsorbent quantities (ranging from 0.3 to 3.0 g L^{-1}), while maintaining consistent conditions for agitation speed (120 rpm), room temperature (25 ± 0.5 °C), adsorbent particle size (90 μm), initial Fe concentration (5.88 mg L^{-1}), and solution pH (7). The percentage of Fe adsorption increased with higher adsorbent doses (Fig. 8). The higher adsorbent doses resulted in an increased number of adsorption sites, contributing to enhanced removal of Fe ions.[30] The optimal adsorbent load for achieving maximum Fe removal was determined to be 3.0 g L^{-1}, attaining a removal efficiency of 88.61%, thereby reducing the Fe concentration to 0.67 mg L^{-1}. Additional increases in baobab seed adsorbent dose did not yield significant improvements, indicating the establishment of equilibrium conditions. This equilibrium point indicates a balance between the adsorption and desorption of Fe, signifying the saturation of the baobab seed adsorbent's capacity.

Effect of solution temperature on Fe removal. Temperature is a highly significant parameter that exerts a dual influence on adsorption, affecting both the kinetics, as it influences the movement of adsorbate molecules within the adsorbent, and the equilibrium aspects by changing the maximum adsorbate capacity of the adsorbent.[3] Experimental investigations at varied temperatures such as (20 °C, 25 °C, 30 °C, 35 °C, 40 °C, 45 °C and 50 °C) were performed under consistent conditions for agitation speed (120 rpm), particle size (90 μm), initial Fe concentration (5.88 mg L^{-1}), and solution pH (7). The results indicated an increasing sorption capacity with higher

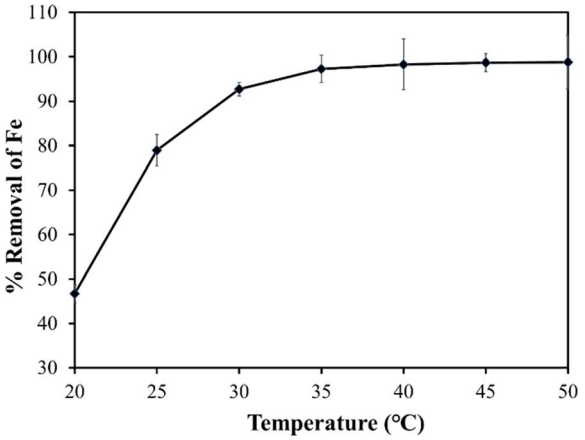

Fig. 9 Effect of solution temperature on Fe removal from groundwater.

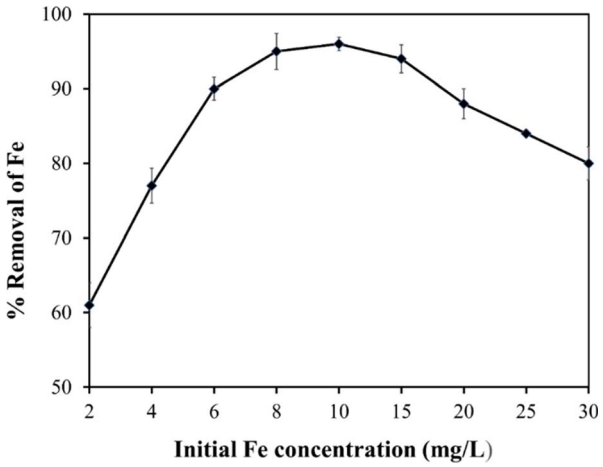

Fig. 10 Effect of the initial metal concentration on Fe removal efficiency.

temperatures peaking at 45 °C with a maximum removal efficiency of 98% (Fig. 9). This temperature-dependent enhancement is attributed to heightened kinetic effects, leading to greater mobility of adsorbate molecules. The observed trend indicates an endothermic and entropy-driven adsorption process.[3] This study aligns with the previous research study reported by (Bayuo *et al.*, 2023)[29] who reported maximum removal efficiency of 95.91% for Hg(II) occurred at 45 °C.

Effect of temperature on thermodynamic parameters. To investigate the thermodynamic properties of the adsorption process, parameters such as the Gibbs free energy (ΔG), enthalpy (ΔH°), and entropy (ΔS°) at various temperatures were calculated.

The results of ΔG obtained from the adsorption experiments are summarized in Table 1.

The results show a clear temperature dependence, with ΔG transitioning from positive values (indicating non-spontaneity) at lower temperatures to negative values (indicating spontaneity) at higher temperatures.[20]

This behaviour suggests that the adsorption process was endothermic, and entropy driven. The increase in temperature provides sufficient thermal energy to overcome the energy barrier for adsorption, and the positive entropy change (ΔS°) contributes significantly to the spontaneity of the process at higher temperatures.[20]

Effect of initial Fe concentration on removal efficiency. The findings depicted in Fig. 10 showcase the outcomes of a research analysis that systematically varied the initial concentrations of Fe in the range of 2 to 30 mg L^{-1}. The results revealed a significant augmentation in the percentage of Fe ion removal by the adsorbent derived from baobab seed, ranging impressively from 61% to 96%.

This observed increase in ion removal can be attributed to a combination of factors such as a heightened driving force and an increased availability of adsorption sites. The higher initial concentrations of Fe create an intensified driving force between the adsorbate and the adsorbent. As the initial adsorbate concentration increases, the driving force for adsorption also intensifies, attracting a greater number of adsorbate molecules to the surface of the adsorbent and enhancing the overall adsorption capacity. These observations align with the findings reported by Vunain *et al.* (2017).[3]

Moreover, at higher initial concentrations, the adsorbent demonstrates an increased availability of adsorption sites. This surplus of available sites results in a higher adsorption capacity, enabling the adsorbent to accommodate a greater quantity of adsorbate molecules. The interplay of an intensified driving force and an increased availability of adsorption sites collectively contributes to the observed escalation in adsorption capacity as initial Fe concentrations increase.

Table 1 Thermodynamic parameters at different temperatures

T (K)	ΔH° (kJ mol^{-1})	ΔS° (kJ mol^{-1})	ΔG (kJ mol^{-1})
293.15	47.78	0.155597	2.16
298.15	47.78	0.155597	1.39
303.15	47.78	0.155597	0.61
308.15	47.78	0.155597	−0.17
313.15	47.78	0.155597	−0.95
318.15	47.78	0.155597	−1.72
323.15	47.78	0.155597	−2.50

Adsorption isotherms

The equilibrium data for synthesized biochar were analysed using both Langmuir and Freundlich models, which are the mathematical frameworks considering factors such as adsorbent homogeneity/heterogeneity, interaction between species, and coverage type, in the adsorption process.[3] These isotherms offer insights into the system's behaviour, adsorbent efficiency, and economic viability. The linear form of the Langmuir isotherm (described by eqn (7)) was employed, and the corresponding plot (Fig. 11) of C_e/q_e (mg g^{-1}) against C_e (mg L^{-1}) was used to determine maximal adsorption capacity (q_m) and adsorption intensity (K_L) based on the slope and intercept of the line.

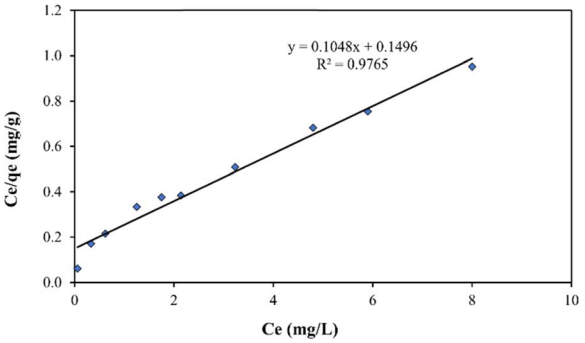

Fig. 11 The Langmuir isotherm plot for Fe removal using baobab seed-derived biochar (adsorbent).

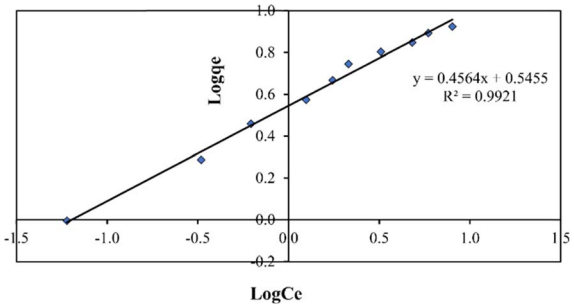

Fig. 12 The Freundlich isotherm plot for Fe removal using baobab seed-derived biochar (adsorbent).

$$\frac{C_e}{q_e} = \frac{1}{q_m K_L} + \frac{1}{q_m} C_e \quad (7)$$

where C_e represents the equilibrium concentration (measured in mg L^{-1}), q_m is the maximum adsorption capacity per unit weight of the adsorbent (measured in mg g^{-1}), K_L is the Langmuir constant indicating the sorption energy between the adsorbate and adsorbent (measured in L mg^{-1}), and q_e denotes the adsorbent's monolayer adsorption capacity (measured in mg g^{-1}).

The derivation of the equilibrium coefficient, specifically the separation factor R_L, was crucial for determining the favourability of the adsorption process. Eqn (8) was employed to achieve this goal. The separation factor R_L is a key parameter used to assess whether the adsorption process is favourable ($R_L < 1$), unfavourable ($R_L > 1$), or approaching irreversibility ($R_L = 1$).[31]

$$R_L = \frac{1}{1 + K_L C_0} \quad (8)$$

where C_0 represents the highest initial concentration of metal in water (mg L^{-1}). In this study, the obtained R_L value was 0.0735, suggesting the favourable adsorption of Fe ions onto the adsorbent surface, as $R_L < 1$. This indicates efficient adsorption performance.

The expression of the Freundlich model is shown in eqn (9):

$$\log q_e = \log K_F + (1/n)\log C_e \quad (9)$$

where C_e is the equilibrium concentration of the adsorbate (mg L^{-1}), q_e is the quantity of metal ions adsorbed at equilibrium (mg g^{-1}), K_F is the Freundlich constant reflecting adsorption capacity, and n is the Freundlich constant representing adsorption intensity. The intercept and slope of a plot showing $\log q_e$ *vs.* $\log C_e$ were used to determine the values of K_F and n (Fig. 12).

The K_F and n values related to the model are displayed in Table 1. According to the model, adsorption is favourable when n exceeds one. The slope $1/n$, ranging from 0 to 1, gauges adsorption intensity or surface heterogeneity; as it nears zero, the surface becomes more heterogeneous.[31]

Both linearized models, Freundlich and Langmuir, demonstrate a satisfactory fit to the experimental data. However, a comparison of their R^2 values from Table 1 suggests that the Freundlich model provides a slightly superior fit compared to the Langmuir isotherm. This implies that the adsorption process within the system is more accurately characterized by a multilayer coverage of the Fe adsorbate on the outer surface of the biochar. Additionally, the Freundlich model suggests that adsorption is taking place on a surface with varying energies or sites, indicating a heterogeneous nature in the adsorption process.

Kinetic models of adsorption

The adsorption of Fe ions onto biochar derived from baobab seeds was investigated using the linear Lagergren pseudo-first-order and pseudo-second-order kinetic models. The primary factor influencing adsorption is the adsorbent's ability to remove heavy metals from water through physicochemical processes. Kinetic studies, including an examination of mechanisms like mass transfer, are essential for understanding the process. To validate the adsorption mechanism, a comparison of the most plausible kinetic models is deemed necessary.[3]

Pseudo-first-order kinetic model. The determination of the adsorption rate constant was done using the pseudo-first-order eqn (10).[32]

$$\frac{dq_e}{dt} = k_1(q_e - q_t) \quad (10)$$

where q_e (mg g^{-1}) represents the amount Fe adsorbed at equilibrium, while q_t (mg g^{-1}) denotes the amount Fe adsorbed at time t (min). The rate constant for the pseudo-first order reaction is denoted as k_1 (per min). When the equation is integrated under the boundary conditions $t = 0$ and $t = t$, $q = q_t$, it establishes the relationship between for the pseudo-first order kinetics and becomes eqn (11):

$$\mathrm{Log}(q_e - q_t) = \log q_e - \left(\frac{k_1}{2.303}\right) t \quad (11)$$

In this study, the determination of the first-order rate constant (k_1) and equilibrium adsorption capacity (q_e) involved analysing the slope and intercepts of a graph, with the obtained values presented in Table 2. However, for the pseudo-first order

Table 2 Parametric values of the adsorption isotherms

Isotherm model	Parameter	Values	R^2
Langmuir	q_m	15.8983	0.9765
	K_L	0.4205	
	R_L	0.0735	
Freundlich	K_f	1.72168	0.9921
	n	2.1911	
	$1/n$	0.4564	

Table 3 Parametric values of each kinetic model

Kinetic model	Parameter	Fitted value
Pseudo-first-order	q_e (exp.) (mg g^{-1})	8.40
	q_e (calc.) (mg g^{-1})	7.82
	K_1 (per min)	0.0138
	R^2	0.9908
Pseudo-second-order	q_e (exp.) (mg g^{-1})	8.40
	q_e (calc.) (mg g^{-1})	8.44
	K_2 (g mg^{-1} min^{-1})	0.0236
	R^2	0.9999

kinetic model, a comparison between the calculated (q_e calc.) and experimental (q_e exp.) values revealed a discrepancy, despite the excellent correlation coefficients (R^2) in Table 3. This inconsistency suggests that the adsorption of Fe did not conform to the pseudo-first-order kinetics.

Pseudo-second-order kinetic model. The study also employed the pseudo-second-order kinetics equation which represents the reaction's rate law, to comprehensively describe the adsorption mechanism of metal ions (specifically Fe) in a solution (water). The kinetic model aims to capture all stages during the adsorption process. The resulting eqn (13), presented in its linear form, was utilized to define the rate law according to ref. 33.

$$\frac{dq_t}{dt} = k_2(q_e - q_t)^2 \quad (12)$$

$$\frac{t}{q_t} = \frac{1}{k_2 q_e^2} + \frac{1}{q_e}t \quad (13)$$

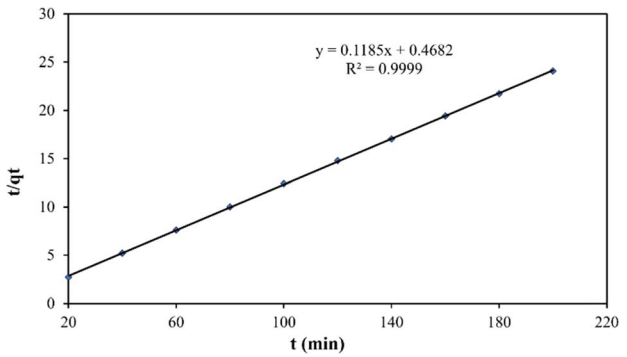

Fig. 13 Pseudo-second-order kinetic plot for the adsorption process using baobab seed-derived biochar.

where the constants k_2 (pseudo-second-order kinetic rate constant) and q_e (adsorption capacity at equilibrium), were determined and presented in Table 3.

The pseudo-second-order plot revealed a linear relationship between $\frac{t}{q_t}$ and t, with k_2 and q_e values obtained from the slope and intercept, respectively, showing high accuracy ($R^2 > 0.99$) (Fig. 13). Calculated q_e values aligned well with experimental data, supporting the conclusion that the adsorption data are effectively represented by pseudo-second-order kinetics. This observation suggests that chemical adsorption is the rate-limiting step, potentially involving ion exchange between the adsorbent and adsorbate Fe ions onto the biochar surface, with chemical bond formation influencing the pseudo-second-order kinetic adsorption.[3]

Conclusions

The assessment of the applicability of low-cost biochar derived from baobab seeds for removing Fe ions from groundwater yielded promising results. The baobab seed-derived biochar as an adsorbent, produced at an optimal pyrolysis temperature of 700 °C, exhibited effective performance across key parameters such as contact time, dose, particle size, solution temperature, and pH. SEM characterization of the material revealed well-developed pores with an irregular shape and a varied size range from micropores to macropores, contributing to the adsorbent's efficacy. The specific surface area of the biochar adsorbent was determined to be 1386.704 m^2 g^{-1}, indicating the presence of a significant surface area and material's ability to adsorb Fe. Furthermore, the same material exhibited exceptional BET characterization, featuring a substantial pore volume of 0.402 cm^3 g^{-1}, and pore radius of 1.5372 nm, enhancing its adsorption capacity.

The adsorption process displayed rapid initial uptake, reaching equilibrium in about 90 minutes. Langmuir isotherm modelling indicated a maximum adsorption capacity of 3.0833 mg g^{-1}, with a favourable adsorption environment suggested by the separation factor (R_L) falling between 0 and 1. Kinetic studies favoured the pseudo-second-order kinetic model as the best fit. These findings underscore the significant potential of baobab seed-derived biochar as an efficient and sustainable adsorbent for Fe removal from groundwater. The study also proposes exploring the development of activated carbon to further enhance the surface area and porosity properties, potentially increasing sorption capacity and extending the applicability of the material to the removal of other divalent metal ions. Further research and field applications are recommended for a comprehensive understanding and optimization of practical implementation including characterization of the adsorbent before and after adsorption to understand any changes in its properties.

Data availability

All data generated or analysed during this study are included in this published article.

Author contributions

All authors contributed to the study conception and design. Magdalena J. Mkelemi and Dr Mwemezi J. Rwiza were responsible for the writing—original draft preparation. Magdalena J. Mkelemi and Dr Grite Nelson Mwaijengo were responsible for the visualization. Drs Mwemezi J. Rwiza and Grite Nelson Mwaijengo were responsible for student project supervision. Magdalena J. Mkelemi, Dr Mwemezi J. Rwiza, and Dr Grite Nelson Mwaijengo were responsible for the data curation. Magdalena J. Mkelemi and Dr Grite Nelson Mwaijengo were responsible for formal analysis and investigation. All the authors worked on the manuscript, read the final version, and approved it.

Conflicts of interest

There are no conflicts to declare.

Acknowledgements

The authors extend their appreciation to the Nelson Mandela African Institution of Science and Technology (NM-AIST) for providing access to research facilities and laboratories. Gratitude is expressed to the Arusha Technical College (ATC) for their support, particularly allowing access to their laboratory and providing equipment such as the Water Jar Test and DR 6000 Spectrophotometer for the determination and treatment of Fe concentrations. The assistance of laboratory technicians from both the NM-AIST and ATC is also acknowledged. The University of Makerere is hereby appreciated for permitting the use of their SEM and XRD instruments for characterization purposes, while the University of Dar es Salaam is recognized for conducting BET characterization on the employed adsorbent in this research study.

References

1 J. Gebauer and E. Luedeling, A note on baobab (Adansonia digitata L.) in Kordofan, Sudan, *Genet. Resour. Crop Evol.*, 2013, **60**, 1587–1596.
2 O. Edogbanya, D. Abolude, M. Adelanwa and O. Ocholi, The Efficacy of the Seeds of Adansonia digitata L. as a Biocoagulant and Disinfectant in Water Purification, *J. Earth Environ. Heath Sci.*, 2016, **2**, 122.
3 E. Vunain, D. Kenneth and T. Biswick, Synthesis and characterization of low-cost activated carbon prepared from Malawian baobab fruit shells by H3PO4 activation for removal of Cu(II) ions: equilibrium and kinetics studies, *Appl. Water Sci.*, 2017, **7**, 4301–4319.
4 G. Sappa, S. Ergul and F. Ferranti, Geochemical modeling and multivariate statistical evaluation of trace elements in arsenic contaminated groundwater systems of Viterbo Area, (Central Italy), *Springerplus*, 2014, **3**, 237.
5 A. bin Jusoh, W. H. Cheng, W. M. Low, A. Nora'aini and M. J. Megat Mohd Noor, Study on the removal of iron and manganese in groundwater by granular activated carbon, *Desalination*, 2005, **182**, 347–353.
6 W. Palmucci, S. Rusi and D. Di Curzio, Mobilisation processes responsible for iron and manganese contamination of groundwater in Central Adriatic Italy, *Environ. Sci. Pollut. Res.*, 2016, **23**, 11790–11805.
7 N. J. Raju, Iron contamination in groundwater: A case from Tirumala-Tirupati environs, India, *The Researcher*, 2006, **1**, 28–31.
8 N. Khatri, S. Tyagi and D. Rawtani, Recent strategies for the removal of iron from water: A review, *J. Water Process Eng.*, 2017, **19**, 291–304.
9 N. El Azher, B. Gourich, C. Vial, M. B. Soulami and M. Ziyad, Study of ferrous iron oxidation in Morocco drinking water in an airlift reactor, *Chem. Eng. Process.*, 2008, **47**, 1877–1886.
10 A. Doggaz, A. Attour, M. Le Page Mostefa, M. Tlili and F. Lapicque, Iron removal from waters by electrocoagulation: Investigations of the various physicochemical phenomena involved, *Sep. Purif. Technol.*, 2018, **203**, 217–225.
11 Q. An, Z. Li, Y. Zhou, F. Meng, B. Zhao, Y. Miao and S. Deng, Ammonium removal from groundwater using peanut shell based modified biochar: Mechanism analysis and column experiments, *J. Water Process Eng.*, 2021, **43**, 102219.
12 K. M. Manjaiah, R. Mukhopadhyay, R. Paul, S. C. Datta, P. Kumararaja and B. Sarkar, in *Modified Clay and Zeolite Nanocomposite Materials*, Elsevier, 2019, pp. 309–329.
13 I. Kithinji Kinoti, J. Ogunah, C. Muturia M'Thiruaine and J. M. Marangu, Adsorption of heavy metals in contaminated water using zeolite derived from agro-wastes and clays: A review, *J. Chem.*, 2022, **1**(2022), 4250299.
14 T. G. Asere, C. V. Stevens and G. Du Laing, Use of (modified) natural adsorbents for arsenic remediation: a review, *Sci. Total Environ.*, 2019, **676**, 706–720.
15 H. Han, M. K. Rafiq, T. Zhou, R. Xu, O. Mašek and X. Li, A critical review of clay-based composites with enhanced adsorption performance for metal and organic pollutants, *J. Hazard Mater.*, 2019, **369**, 780–796.
16 N. M. Mubarak, J. N. Sahu, E. C. Abdullah and N. S. Jayakumar, Removal of Heavy Metals from Wastewater Using Carbon Nanotubes, *Separ. Purif. Rev.*, 2013, **43**, 311–338.
17 J. B. Njewa and V. O. Shikuku, Recent advances and issues in the application of activated carbon for water treatment in Africa: a systematic review (2007–2022), *Appl. Surf. Sci. Adv.*, 2023, **18**, 100501.
18 N. Ayawei, A. N. Ebelegi and D. Wankasi, Modelling and interpretation of adsorption isotherms, *J. Chem.*, 2017, **2017**, 3039817.
19 R. A. Tabassum, M. Shahid, N. K. Niazi, C. Dumat, Y. Zhang, M. Imran, H. F. Bakhat, I. Hussain and S. Khalid, Arsenic removal from aqueous solutions and groundwater using agricultural biowastes-derived biosorbents and biochar: a column-scale investigation, *Int. J. Phytorem.*, 2019, **21**, 509–518.
20 O. R. Obanla, J. A. Hestekin, M. E. Ojewumi, I. Bousrih and M. C. Fawole, Enhancing rubber (Hevea brasiliensis) seed

shell biochar through acid-base modification for effective phenol removal from aqueous environments, *Results Eng.*, 2023, **20**, 101584.

21 A. M. Ealias and M. Saravanakumar, Facile synthesis and characterisation of AlNs using Protein Rich Solution extracted from sewage sludge and its application for ultrasonic assisted dye adsorption: Isotherms, kinetics, mechanism and RSM design, *J. Environ. Manage.*, 2018, **206**, 215–227.

22 O. M. Siddiq, B. S. Tawabini, P. Soupios and D. Ntarlagiannis, Removal of arsenic from contaminated groundwater using biochar: a technical review, *Int. J. Environ. Sci. Technol.*, 2021, **19**, 651–664.

23 N. K. Kalagatur, K. Karthick, J. A. Allen, O. S. Nirmal Ghosh, S. Chandranayaka, V. K. Gupta, K. Krishna and V. Mudili, Application of Activated Carbon Derived from Seed Shells of Jatropha curcas for Decontamination of Zearalenone Mycotoxin, *Front. Pharmacol.*, 2017, **8**, 760.

24 T. Bohli, A. Ouederni, N. Fiol and I. Villaescusa, Evaluation of an activated carbon from olive stones used as an adsorbent for heavy metal removal from aqueous phases, *C. R. Chim.*, 2014, **18**, 88–99.

25 A. M. Ealias and M. P. Saravanakumar, Application of protein-functionalised aluminium nanosheets synthesised from sewage sludge for dye removal in a fixed-bed column: Investigation on design parameters and kinetic models, *Environ. Sci. Pollut. Res.*, 2020, **27**, 2955–2976.

26 H. N. Tran, S.-J. You and H.-P. Chao, Fast and efficient adsorption of methylene green 5 on activated carbon prepared from new chemical activation method, *J. Environ. Manage.*, 2017, **188**, 322–336.

27 R. H. Krishna and A. Swamy, Physico-Chemical Key Parameters, Langmuir and Freundlich isotherm and Lagergren Rate Constant Studies on the removal of divalent nickel from the aqueous solutions onto powder of calcined brick, *Int. J. Eng. Res. Dev.*, 2012, **4**, 29–38.

28 N. Priyadarshni, P. Nath, Nagahanumaiah and N. Chanda, Sustainable removal of arsenate, arsenite and bacterial contamination from water using biochar stabilized iron and copper oxide nanoparticles and associated mechanism of the remediation process, *J. Water Process Eng.*, 2020, **37**, 101495.

29 J. Bayuo, M. J. Rwiza and K. M. Mtei, Modeling and optimization of trivalent arsenic removal from wastewater using activated carbon produced from maize plant biomass: a multivariate experimental design approach, *Convers. Biorefin.*, 2023, **14**(2024), 24809–24832.

30 L. Verma and J. Singh, Synthesis of novel biochar from waste plant litter biomass for the removal of Arsenic (III and V) from aqueous solution: A mechanism characterization, kinetics and thermodynamics, *J. Environ. Manage.*, 2019, **248**, 109235.

31 E. Vunain, A. K. Mishra and R. W. Krause, Ethylene-vinyl acetate (EVA)/polycaprolactone (PCL)–Fe3O4 composites, *Therm. Anal. Calorim.*, 2013, **114**, 791–797.

32 A. A. Rahim and Z. N. Garba, Efficient adsorption of 4-Chloroguiacol from aqueous solution using optimal activated carbon: Equilibrium isotherms and kinetics modeling, *J. Assoc. Arab Univ. Basic Appl. Sci.*, 2016, **21**, 17–23.

33 Y. S. Ho and G. McKay, Pseudo-second order model for sorption processes YS, *Process Biochem.*, 1999, **34**, 451–465.